

**Chirality-dependent growth rate of carbon nanotubes: A theoretical study**

Heiko Dumlich\* and Stephanie Reich

*Fachbereich Physik, Freie Universität Berlin, 14195 Berlin, Germany*

(Received 16 April 2010; revised manuscript received 30 June 2010; published 12 August 2010)

We consider geometric constraints for the addition of carbon atoms to the rim of a growing nanotube. The growth of a tube proceeds through the conversion of dangling bonds from armchair to zigzag and vice versa. We find that the growth rate depends on the rim structure (chirality), the energy barriers for dangling-bond conversion, and the growth temperature. A calculated chirality distribution derived from this minimalistic theory shows surprisingly good agreement with experiment. Our ideas imply that the chirality distribution of carbon nanotubes can be influenced by external parameters.

DOI: [10.1103/PhysRevB.82.085421](https://doi.org/10.1103/PhysRevB.82.085421)

PACS number(s): 61.48.De, 61.46.Fg, 81.07.De, 81.10.Aj

**I. INTRODUCTION**

The properties of carbon nanotubes<sup>1</sup> depend strongly on their chirality or atomic structure. Most notably, the metallic and semiconducting character and the band gap of a tube change with  $(n, m)$  chiral index. One of the greatest challenges in nanotube research and application is to control the chirality during the growth. This would allow the production of tubes with tailored properties without relying on a sorting of bulk samples.

The growth of a nanotube can conceptually be divided into two stages: the nucleation of a cap and the elongation of the nucleus into a tube.<sup>2–6</sup> Reich *et al.*<sup>7</sup> showed that the nucleation of the cap fixes the chirality of an individual tube as a change in chirality is unlikely during the growth phase. Harutyunyan *et al.*<sup>8</sup> reported preferential growth of metallic tubes and claimed the selection to follow from the shape of the catalytic particles, i.e., chirality selection during the nucleation phase.

The final volume fraction of a given nanotube type does not only depend on the nucleation but also on growth speed during elongation. Elongation was mainly studied in simplistic models with carbon addition.<sup>9,10</sup> Ding *et al.*<sup>11</sup> argued that achiral armchair and zigzag tubes grow by introducing kinks when starting a new layer. They predicted the armchair kinks to require much less energy than zigzag kinks. The growth process, which is driven by a monotonous decrease in free energy during elongation, will, therefore, favor armchair tubes. Within this line of reasoning chirality selection is independent of external parameters such as catalyst type and temperature.

In this paper, we suggest that the chiral-angle distribution of carbon nanotubes depends on external parameters. The key is to manipulate the energy difference between armchair and zigzag dangling bonds through the choice of metal catalyst and growth conditions. We arrive at this conclusion by looking at the geometry of a growing tube, the number and types of places for carbon addition. The rim of a nanotube consists of three different growth sites with a varying energy barrier for the addition of carbon atoms. The number and distribution of growth sites is a function of chirality. Combining this minimalistic geometric approach with calculated energy differences for carbon dangling bonds on metals, we predict a distribution of chiral angles that is in surprisingly good agreement with experimental findings.

This paper is organized as follows. We first show how growth proceeds with carbon addition with respect to our model, Sec. II A. The essential properties of rims made up by hexagons are discussed in Sec. II B. The growth factor, which allows us to understand why chiral selectivity occurs during the nanotube elongation, is introduced in Sec. II C. We then discuss how the chirality distribution can be influenced by external parameters in Sec. II D. Finally, in Sec. III we use our model—derived in Sec. II—to obtain two exemplary chirality distributions and compare our results to experimentally determined data. Section IV summarizes this work.

**II. MODEL****A. Growth**

Let us first consider schematically the growth of a carbon nanotube. In Fig. 1 we present a three-dimensional (3D) wire model of a possible growth route of a (5,5) nanotube. The growth proceeds through to addition of  $C_2$ . The first carbon atom adds endothermically and is followed exothermically by a second carbon atom. The pentagon created in the first step is energetically less favorable than hexagons. We, therefore, expect the next carbon atom to be added to the pentagon. Also, the creation of more and more pentagons would close the tube and terminate growth.<sup>12</sup> Alternatively, a carbon dimer is added.

Going through the series of tubes in Figs. 1(a)–1(d) a layer of carbon atoms was grown, which corresponds to half a unit cell of the (5,5) tube. The continuation of the process—until growth is terminated—leads to an armchair carbon nanotube. In the lower panels of Figs. 1(a)–1(d) we introduce a schematic representation of the growing rim of a nanotube. The reduced rim representation unfolds the rim of the tubes in two dimensions. The “.” denotes growth sites at which the addition of  $C_2$  is energetically favorable because a hexagon is created. The  $a$  stands for an armchair dangling bond; it consists of one of two neighboring twofold C-C bonded atoms. The  $z$  stands for zigzag dangling bond; it has two saturated C neighbors and is itself twofold C-C bonded.

The first  $C_2$  addition to the rim starts a new layer by converting two  $a$  into  $z$  dangling bonds, which is accompanied by an energy barrier,<sup>11</sup> compare Figs. 1(a) and 1(b). The



$$\Lambda_{aa,aa}(n,m) = 2m - n - 1 + \frac{1}{2m - n}. \quad (1)$$

Similarly, we find the average growth site number for the rim part containing  $aa.z$  sites  $\Lambda_{aa,z} = N_{aa,z}$ . Adding the contributions of  $aa,aa$  and  $aa.z$  rim parts yield the average number of growth sites as a function of chiral indexes  $n$  and  $m$ ,

$$\Lambda(n,m) = \begin{cases} \Lambda_{aa,aa} + \Lambda_{aa,z} & \text{if } 2m - n > 0 \\ \Lambda_{aa,z} & \text{otherwise.} \end{cases} \quad (2)$$

The addition of  $C_2$  dimers to the  $\Lambda(n,m)$  sites will lead to a lengthening of the tube with  $n+m$   $C_2$  additions for a single full layer. If we define the abundance of a certain nanotube chirality to depend on the number of full carbon layers, we find the growth speed of a tube to be proportional to

$$\Gamma(n,m) = \frac{\Lambda(n,m)}{n+m}. \quad (3)$$

The growth factor  $\Gamma(n,m)$  allows us to understand why chiral selectivity occurs during the nanotube elongation phase. In the following we will show how we can influence the chiral distribution during the elongation of a nanotube.

#### D. Influence on chirality distribution

The addition of  $C_2$  to the different growth sites will experience varying energy barriers, as zigzag dangling bonds ( $E_z = 2.90$  eV) require much more energy than armchair dangling bonds ( $E_a = 2.10$  eV) in vacuum.<sup>14</sup> The armchair configuration is energetically favorable because it consists of two dangling bonds on neighboring C atoms that form a triple bond. To model experimental growth conditions we need to consider a metal catalyst in most growth scenarios. The energetic difference between  $a$  and  $z$  dangling bonds is reduced by the presence of a metal,<sup>6,7,11</sup> as carbon-metal bonds are formed. However, the difference remains nonzero, as electrons of carbon neighbors influence the total bond energy of the carbon-metal bonds, rendering  $a$  lower in energy than  $z$ .

The energy barrier for the  $C_2$  addition to an  $aa,aa$  site depends on the conversion of  $aa,aa$  into  $zaaz$  dangling bonds (see Table I). The conversion requires an energy

$$\Delta_a = E_{zaaz} - E_{aa,aa} = 2E_z - 2E_a = 2E_a(r - 1) \quad (4)$$

with  $E_a$  the energy of an armchair and  $E_z$  the energy of a zigzag dangling bond. With  $r = E_z/E_a$  we denote the ratio between the two energies. The total dangling-bond energies as well as their ratio depend on the catalyst. Changing  $z.z$  into  $.aa.$  we gain  $\Delta_a$ . In contrast growing at an  $aa.z$  site will cost no energy; this growth happens without an energetic barrier. This energetically different behavior allows to affect the chirality distribution of carbon nanotubes through external parameters such as the metal catalyst and the growth temperature.

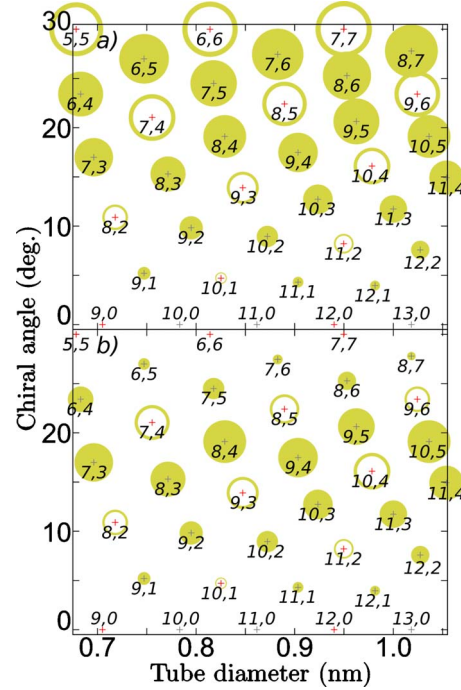


FIG. 2. (Color online) Comparison of  $\Gamma(n,m)$  for tube diameters  $d=0.675-1.055$  nm for (a)  $\Delta_a \ll k_B T$ , and (b)  $\Delta_a \gg k_B T$ . The abundance of metallic/semimetallic tubes (open circle, red cross) decreases compared to semiconducting tubes (full circle, gray cross) from (a) to (b).

If the addition to  $aa,aa$  sites has a negligible barrier ( $r \approx 1$  or  $\Delta_a \ll k_B T$ ) all growth sites can contribute to the growth speed. We combine Eqs. (2) and (3) to obtain  $\Gamma$ . Figure 2(a) shows the growth speed  $\Gamma$  as area size in chiral angle and diameter dependence for diameters  $d=0.675-1.055$  nm. The highest  $\Gamma$  occur for  $(n,n)$  armchair tubes. A small trend for increasing  $\Gamma$  exists for larger diameter tubes, resulting from the fractional term of Eq. (1), as the comparison of the armchair tubes shows. Changing the environment (e.g., another catalyst with another  $r$  or adjustment of temperature) so that  $\Delta_a \gg k_B T$ , the  $aa,aa$  growth sites will not contribute anymore; Eq. (3) yields  $\Gamma = \Lambda_{aa,z}/(n+m)$ , which leads to a different growth speed distribution. The highest  $\Gamma$  now occurs for  $(n, \frac{n}{2})$  chiral tubes, see Fig. 2(b).

For real samples we expect a distribution of growth speed  $\Gamma$  to be between the two limiting cases. The thermal energy of nanotube growth is on the order of  $k_B T \approx 0.05-0.11$  eV.<sup>15,16</sup>  $\Delta_a$  depends on the catalyst material, its composition and—less pronounced—on the position of the carbon with respect to the metal atom. The barriers for metal catalysts are on the order of  $\Delta_a \approx 0-0.12$  eV for various metals<sup>7,11</sup> and thus comparable to the thermal energy. Therefore, the addition to the  $aa,aa$  site is not suppressed. This agrees with the results of Ding *et al.*<sup>11</sup> that the barrier for armchair kink introduction—which corresponds to  $C_2$  addition to  $aa,aa$ —is negligible. Recently, other materials such as  $SiO_2$  were found to catalyze nanotube growth.<sup>17</sup> Further, bimetallic catalysts contain different barriers and may be extremely interesting for influencing the chirality distribution.<sup>18</sup>

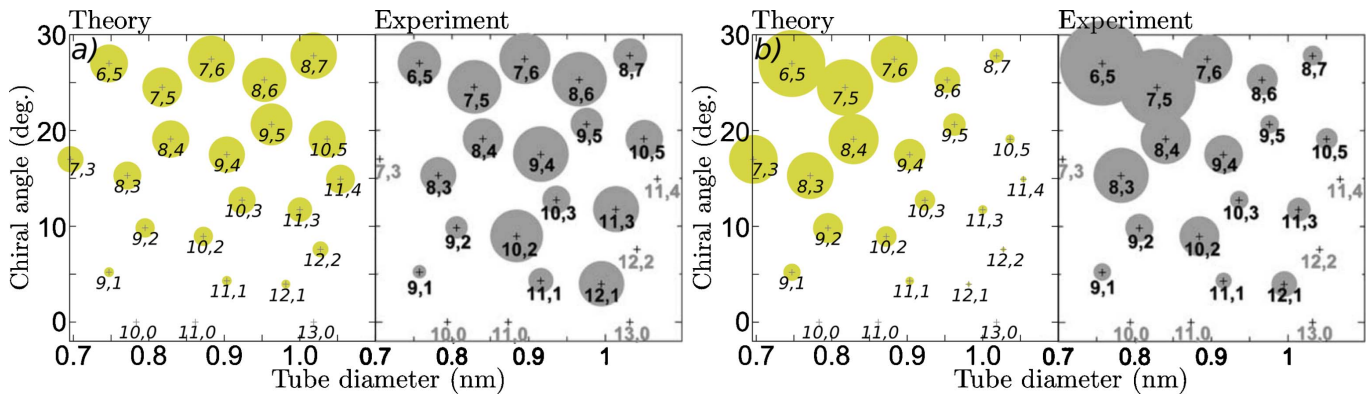


FIG. 3. (Color online) Comparison of chirality distributions. Theoretically calculated distributions result from a convolution of a Gaussian distribution in diameter dependence and the  $\Gamma$  factor for  $\Delta_a \ll k_B T$ . The experimentally determined chirality distributions are adapted from Miyachi *et al.* (Ref. 21). (a) Theory:  $d = (0.93 \pm 0.3)$  nm (Ref. 22). Experiment: HiPco sample. (b) Theory:  $d = (0.75 \pm 0.15)$  nm. Experiment: ACCVD sample grown at 650 °C with Fe/Co catalyst.

### III. DISCUSSION

Up to now we concentrated on the growth of an existing nanotube nucleus. The chirality distribution of a sample will also depend on the nucleation phase, i.e., whether a particular tube cap is nucleated or not.<sup>19</sup> The diameter of carbon nanotubes is clearly determined by the nucleation step.<sup>20</sup> We now assume a distribution of chiral indices where (i) the diameter is fixed by nucleation and (ii) the chiral-angle distribution is given by Eq. (3) with  $\Delta_a \ll k_B T$ . Figure 3(a) compares the chirality distribution of semiconducting nanotubes with  $d = (0.93 \pm 0.3)$  nm to the experimental distribution in HiPco tubes; Fig. 3(b) is for tubes with  $d = (0.75 \pm 0.15)$  nm and samples produced by alcohol catalytic chemical vapor deposition (ACCVD) (see Ref. 21). The agreement between theory and experiment in Fig. 3(b) is striking. Our model very well predicts the overall decrease in the number of tubes with increasing chiral angle. The strong discrepancies for selected chiralities—e.g., the strong luminescence of the (10,2) tube—is most likely due to a high quantum yield for some nanotubes.<sup>23</sup> On the other hand, the nucleation phase might also prefer certain chiralities.<sup>7</sup> It would be highly desirable to establish an unambiguous chirality distribution experimentally to clarify these points.

Figure 3(a) verifies our assumption that a mixture of the  $\Gamma$  factors derived for  $\Delta_a \ll k_B T$  and  $\Delta_a \gg k_B T$  have to be used for

real samples as the deviation between the theoretical and experimental part of Fig. 3(a) show. Figure 3(b) on the other hand perfectly reproduces the trend with only considering the contribution of the  $\Gamma$  factor for  $\Delta_a \ll k_B T$ , which is expected to result from the growth conditions. We conclude that different growth conditions have indeed an influence on the chirality distributions which results during the elongation of the nanotubes.

### IV. CONCLUSIONS

In summary, we suggested how to control the nanotube growth and elongation process through the structure of the rim. Depending on the tube chirality the rim contains three different growth sites. Geometric considerations yield the growth factor  $\Gamma$ , which in turn determines the chirality distribution of carbon nanotube samples. We showed that chiral selectivity can be obtained through a combination of external parameters. Our results will be important for the understanding and tailoring of the growth process of single-walled carbon nanotubes.

### ACKNOWLEDGMENTS

We acknowledge useful discussions with J. Robertson and S. Heeg. This work was supported by ERC under Grant No. 210642.

\*Corresponding author; heiko.dumlich@fu-berlin.de

<sup>1</sup>S. Iijima and T. Ichihashi, *Nature (London)* **363**, 603 (1993).

<sup>2</sup>H. Amara, C. Bichara, and F. Ducastelle, *Phys. Rev. Lett.* **100**, 056105 (2008).

<sup>3</sup>Y. Ohta, Y. Okamoto, A. J. Page, S. Irlle, and Keiji Morokuma, *ACS Nano* **3**, 3413 (2009).

<sup>4</sup>J.-Y. Raty, F. Gygi, and G. Galli, *Phys. Rev. Lett.* **95**, 096103 (2005).

<sup>5</sup>X. Fan, R. Buczko, A. A. Puretzky, D. B. Geohegan, J. Y. Howe, S. T. Pantelides, and S. J. Pennycook, *Phys. Rev. Lett.* **90**,

145501 (2003).

<sup>6</sup>O. V. Yazyev and A. Pasquarello, *Phys. Rev. Lett.* **100**, 156102 (2008).

<sup>7</sup>S. Reich, L. Li, and J. Robertson, *Chem. Phys. Lett.* **421**, 469 (2006).

<sup>8</sup>A. R. Harutyunyan, G. Chen, T. M. Paronyan, E. M. Pigos, O. A. Kuznetsov, K. Hewaparakrama, S. M. Kim, D. Zakharov, E. A. Stach, and G. U. Sumanasekera, *Science* **326**, 116 (2009).

<sup>9</sup>D. A. Gómez-Gualdrón and P. B. Balbuena, *Nanotechnology* **19**, 485604 (2008).

- <sup>10</sup>Q. Wang, M.-F. Ng, S.-W. Yang, Y. Yang, and Y. Chen, *ACS Nano* **4**, 939 (2010).
- <sup>11</sup>F. Ding, A. R. Harutyunyan, and B. I. Yakobson, *Proc. Natl. Acad. Sci. U.S.A.* **106**, 2506 (2009).
- <sup>12</sup>Y. H. Lee, S. G. Kim, and D. Tomanek, *Phys. Rev. Lett.* **78**, 2393 (1997).
- <sup>13</sup>The number of growth sites for other, less likely growth paths will differ somewhat from Eq. (1). However, we verified Eq. (1) to be correct within  $\pm 5\%$  [derived for the (4,4) tube in comparison to the next four less likely paths].
- <sup>14</sup>A. Thess, R. Lee, P. Nikolaev, H. Dai, P. Petit, J. Robert, C. Xu, Y. H. Lee, S. G. Kim, A. G. Rinzler, D. T. Colbert, G. E. Scuseria, D. Tomanek, J. E. Fischer, and R. E. Smalley, *Science* **273**, 483 (1996).
- <sup>15</sup>M. Cantoro, S. Hofmann, S. Pisana, V. Scardaci, A. Parvez, C. Ducati, A. C. Ferrari, A. M. Blackburn, K.-Y. Wang, and John Robertson, *Nano Lett.* **6**, 1107 (2006).
- <sup>16</sup>L. Zheng, B. C. Satishkumar, P. Gao, and Q. Zhang, *J. Phys. Chem. C* **113**, 10896 (2009).
- <sup>17</sup>B. Liu, W. Ren, C. Liu, C.-H. Sun, L. Gao, S. Li, C. Jiang, and H.-M. Cheng, *ACS Nano* **3**, 3421 (2009).
- <sup>18</sup>W.-H. Chiang and R. M. Sankaran, *Nature Mater.* **8**, 882 (2009).
- <sup>19</sup>S. Reich, L. Li, and J. Robertson, *Phys. Rev. B* **72**, 165423 (2005).
- <sup>20</sup>Y. Li, W. Kim, Y. Zhang, M. Rolandi, D. Wang, and H. Dai, *J. Phys. Chem. B* **105**, 11424 (2001).
- <sup>21</sup>Y. Miyauchi, S. Chiashi, Y. Murakami, Y. Hayashida, and S. Maruyama, *Chem. Phys. Lett.* **387**, 198 (2004).
- <sup>22</sup>S. M. Bachilo, M. S. Strano, C. Kittrell, R. H. Hauge, R. E. Smalley, and R. B. Weisman, *Science* **298**, 2361 (2002).
- <sup>23</sup>S. Reich, C. Thomsen, and J. Robertson, *Phys. Rev. Lett.* **95**, 077402 (2005).